BIOCHEMISTRY
including biophysical chemistry & molecular biology

Article

pubs.acs.org/biochemistry

Kinetic Analysis of a Globin-Coupled Histidine Kinase, *Af*GcHK: Effects of the Heme Iron Complex, Response Regulator, and Metal Cations on Autophosphorylation Activity

Veronika Fojtikova,[†] Martin Stranava,[†] Marten H. Vos,[§] Ursula Liebl,[§] Jakub Hranicek,[‡] Kenichi Kitanishi,[†] Toru Shimizu,[†] and Marketa Martinkova*[,†]

[†]Department of Biochemistry and [‡]Department of Analytical Chemistry, Faculty of Science, Charles University in Prague, Hlavova (Albertov) 2030-8, Prague 2, Czech Republic

[§]Laboratoire d'Optique et Biosciences, INSERM U1182-CNRS UMR7645, Ecole Polytechnique, 91128 Palaiseau Cedex, France

Supporting Information

ABSTRACT: The globin-coupled histidine kinase, *Af*GcHK, is a part of the two-component signal transduction system from the soil bacterium *Anaeromyxobacter* sp. Fw109-5. Activation of its sensor domain significantly increases its autophosphorylation activity, which targets the His183 residue of its functional domain. The phosphate group of phosphorylated *Af*GcHK is then transferred to the cognate response regulator. We investigated the effects of selected variables on the autophosphorylation reaction's kinetics. The k_{cat} values of the heme Fe(III)-OH^-, Fe(III)-cyanide, Fe(III)-imidazole, and Fe(II)-O_2 bound active *Af*GcHK forms were 1.1−1.2 min^{-1}, and their K_m^{ATP} values were 18.9−35.4 μM. However, the active form bearing a CO-bound Fe(II) heme had a k_{cat} of 1.0 min^{-1} but a very high K_m^{ATP} value of 357 μM, suggesting that its active site structure differs strongly from the other active forms. The Fe(II) heme-bound inactive form had k_{cat} and K_m^{ATP} values of 0.4 min^{-1} and 78 μM, respectively, suggesting that its low activity reflects a low affinity for ATP relative to that of the Fe(III) form. The heme-free form exhibited low activity, with k_{cat} and K_m^{ATP} values of 0.3 min^{-1} and 33.6 μM, respectively, suggesting that the heme iron complex is essential for high catalytic activity. Overall, our results indicate that the coordination and oxidation state of the sensor domain heme iron profoundly affect the enzyme's catalytic activity because they modulate its ATP binding affinity and thus change its k_{cat}/K_m^{ATP} value. The effects of the response regulator and different divalent metal cations on the autophosphorylation reaction are also discussed.

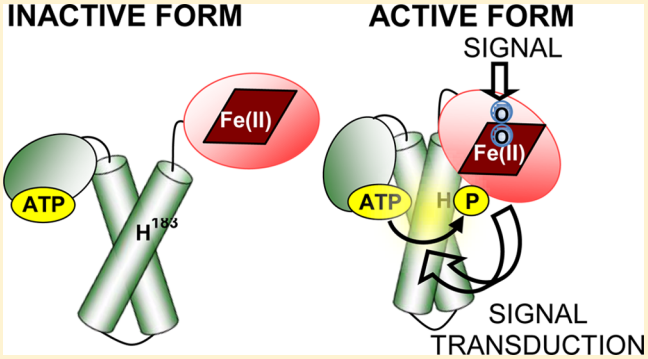

The ability to sense environmental changes is important for all organisms. In particular, it is important to detect changes in the concentration of the physiologically most important gas, O_2, and other gases such as CO and NO, as well. Heme iron complexes have been shown to play central roles in gas sensing.[1] Heme-containing sensor proteins generally consist of two domains: an N-terminal sensor domain containing the heme-based gas-sensing site and a C-terminal functional domain. The structure−function relationship and mechanisms of communication between these domains have not yet been resolved in detail. DNA sequencing has revealed thousands of heme-binding domains (motifs and proteins) in the genomes of various organisms,[2] demonstrating their physiological importance and emphasizing the need for a detailed understanding of their mechanisms of action and the structure−function relationships of their domains.

One subgroup of heme-containing oxygen sensor proteins features functional domains that exhibit histidine kinase activity. Several such proteins have recently been characterized.[3−14] Histidine kinases are the first components of the two-component signal transduction systems found in bacteria; the second components are the response regulator (RR) proteins.[15−17] In general, sensor kinases are multidomain proteins containing a nonconserved sensory input domain responsible for detecting a particular stimulus or ligand and a conserved kinase domain.[15−18] RRs are also multidomain proteins with a conserved receiver domain and a variable output domain.[19−21] Once the sensor domain of a histidine kinase is activated by the first signal, the functional domain is stimulated and the autophosphorylation of a conserved His residue in the functional domain can be observed. This phosphate group is subsequently transferred to a conserved Asp residue in the receiver domain of the cognate RR, activating its output domain.

The most extensively characterized heme-containing oxygen sensor histidine kinases are FixL,[5,6] DosT,[8−11] and DevS (DosS).[8−11] FixL is involved in regulating the expression of

Received: May 11, 2015
Revised: July 2, 2015
Published: July 25, 2015

DOI: 10.1021/acs.biochem.5b00517
Biochemistry 2015, 54, 5017−5029

genes essential for nitrogen fixation and the anaerobic respiratory chain in root nodule bacteria such as *Rhizobium meliloti*.[5,6] DosT and DevS are enzymes from *Mycobacterium tuberculosis* that regulate the expression of genes necessary for survival under hypoxic conditions.[8−11] A new member of the heme-containing oxygen sensor histidine kinase family was recently discovered, a globin-coupled histidine kinase known as *Af*GcHK from the soil bacterium *Anaeromyxobacter* sp. Fw109-5.[14] Although oxygen sensor histidine kinases with heme-bound PAS folds (FixL) or GAF folds (DosS, DosT) are known and have been well-characterized, *Af*GcHK is the first oxygen sensor histidine kinase that contains a heme-bound globin fold and is involved in a two-component signaling system. *Af*GcHK is also distinctive in that its catalytic activity is stimulated by the binding of O_2 to its heme Fe(II) complex, whereas the catalytic activity of FixL and DosS/DosT is stimulated by the dissociation of O_2 from the heme Fe(II) complex.[22] *Af*GcHK has already been partially characterized,[14] but many questions regarding its function and mechanism of action remain unresolved. In particular, its mechanism of action is poorly understood because it is not clear how signals are transduced between the sensor and functional domains. Two-component signaling has been linked to biofilm formation and virulence in certain pathogenic bacteria, making the components of these signaling systems attractive targets for controlling and suppressing these pathological processes. However, to control the function of these proteins, we must understand molecular mechanisms of their action. This work sheds new light on the process of signal transduction between the sensor and functional domains of a model heme-containing sensor protein.

It has been suggested that unlike well-known oxygen storage hemoproteins such as myoglobin, the heme-containing sensor proteins require a degree of structural flexibility to be functional.[23−25] However, their structures and the global conformational changes induced by changes in the redox state or coordination of the heme iron have been characterized using only indirect experimental methods, while X-ray crystallographic data for only a few isolated sensor and/or functional domains of certain heme-based gas sensor proteins have been obtained, there are currently no X-ray crystal structures for any full-length heme-based oxygen sensor protein[26,27] and only one such structure for a full-length heme-based CO sensor protein.[27] The lack of robust structural data makes it challenging to explain the general relationships among signal transduction, protein conformation, and the functional state of these sensor proteins. However, an understanding of these relationships is required to effectively manipulate their behavior.

To address this knowledge gap, we investigated the full-length heme-based gas sensor protein *Af*GcHK. The interactions between its sensor and functional domains were probed by performing kinetic analyses of its autophosphorylation activity under diverse conditions. Specifically, we studied the impact of changes in the heme iron's redox state as well as the effects of various ligands, the RR protein, and different metal cations on the autophosphorylation activity of the *Af*GcHK functional domain.

EXPERIMENTAL PROCEDURES

Materials. Ampicillin was obtained from P-lab (Prague, Czech Republic). Isopropyl β-D-thiogalactopyranoside, hemin, and acrylamide were obtained from Sigma-Aldrich (St. Louis, MO). Water, doubly distilled over quartz, was purified using a Milli-Q Plus system (EMD Millipore, Billerica, MA). All glassware used for sample preparation was conditioned in advance by being allowed to stand for 24 h in 10% HCl suprapur (Merck, Darmstadt, Germany). Phos-tag was from the Phos-tag consortium Wako Pure Chemical Industries (Osaka, Japan). All chemicals used were of the highest purity grade available from commercial sources and used without further purification.

Overexpression and Purification of the Wild-Type and Mutant Proteins. Cloning, site-directed mutagenesis, overexpression in *Escherichia coli*, and purification of His tagged-*Af*GcHK were performed in a manner slightly different from that of the experiments previously described.[14] The full-length wild-type and His99Ala proteins were prepared as described below. Briefly, *E. coli* BL21(DE3) (Novagen) was transformed with the appropriate pET 21c(+) plasmid, plated on LB agar containing 100 μg mL^{-1} ampicillin, and incubated at 37 °C overnight. The following day, a single colony was inoculated in LB medium containing 100 μg mL^{-1} ampicillin and shaken overnight at 250 rpm and 37 °C. The culture medium was then added to fresh Terrific Broth (1:1000 dilution) containing the same antibiotic concentration, and the mixture was again shaken at 250 rpm and 37 °C for 4 h. Subsequently, the medium was cooled to 15 °C, and protein expression was induced by the addition of 0.1 mM isopropyl β-D-thiogalactopyranoside followed by further shaking for 20 h. The *E. coli* cells were harvested by centrifugation for 30 min at 5000*g* and 4 °C, frozen in liquid nitrogen, and stored at −80 °C until the protein was purified. Frozen pellet cells were resuspended in buffer A [50 mM Tris-HCl (pH 8.0) and 100 mM NaCl] containing 1 mM phenylmethanesulfonyl fluoride and 1 mM ethylenediaminetetraacetic acid and lysed with 0.2 mg mL^{-1} lysozyme. The crude extract was sonicated six times for 1 min each (with 1 min intervals between sonications) on ice and then centrifuged at 50000*g* for 60 min at 4 °C. The resulting supernatant was incubated for 20 min with or without (in the case of the His99Ala mutant) hemin in dimethyl sulfoxide (300 μM) and then applied to a TALON Metal Affinity Resin column (Clontech Laboratories) that had been pre-equilibrated with buffer A. The column was then washed with buffer A containing 20 mM imidazole, and *Af*GcHK fractions were eluted with a linear gradient from 20 to 200 mM imidazole in buffer A. Protein fractions were pooled and applied to a Superdex 200 10/300 GL column (GE Healthcare) equilibrated with 20 mM Tris-HCl pH 8.0 buffer containing 150 mM NaCl. The desired eluates (identified by monitoring at 280 nm) were collected and concentrated with Amicon Ultra Centrifugal Filters (Millipore). Finally, the purified proteins were quickly frozen in liquid nitrogen and stored at −80 °C. Protein and heme concentrations were determined using the bicinchoninic acid assay with bovine serum albumin as a standard (Sunrise Absorbance Reader, TECAN) and the pyridine hemochromogen assay, respectively.[28] Purified proteins were >90% homogeneous, as confirmed by polyacrylamide gel electrophoresis in the presence of sodium dodecyl sulfate (SDS−PAGE).

The apo form of the WT *Af*GcHK protein was prepared by omitting the incubation with hemin during the purification process and by removing the residual heme iron complex from the expression process using the previously reported procedure.[29]

Cloning, site-directed mutagenesis, overexpression in *E. coli*, and purification of GST-tagged RR were performed in a

DOI: 10.1021/acs.biochem.5b00517
Biochemistry 2015, 54, 5017−5029

manner slightly different from that of the experiments previously described.[14] The full-length wild-type and Asp52/169Ala mutant RR were prepared as described below. Briefly, *E. coli* BL21(DE3) cells (Novagen) were transformed with the corresponding pGEX-6P-2 expression vector, plated on LB agar containing 100 μg mL^{-1} ampicillin, and incubated at 37 °C overnight. The following day, a single colony was inoculated in LB medium containing 100 μg mL^{-1} ampicillin and shaken overnight at 250 rpm and 37 °C. The culture medium was then added to fresh Terrific Broth (1:1000 dilution) containing the antibiotic mentioned above, and the mixture was again shaken at 250 rpm and 37 °C for 4 h. Subsequently, the medium was cooled to 15 °C, and protein expression was induced by the addition of 0.1 mM isopropyl β-D-thiogalactopyranoside followed by further shaking for 20 h. The *E. coli* cells were harvested by centrifugation for 30 min at 5000*g* and 4 °C, frozen in liquid nitrogen, and stored at −80 °C until the protein was purified. *E. coli* cells were resuspended in buffer B [10 mM Na_2HPO_4, 1.8 mM KH_2PO_4 (pH 7.5), 140 mM NaCl, and 2.7 mM KCl] with 1 mM ethylenediaminetetraacetic acid, 1 mM phenylmethanesulfonyl fluoride, and 0.2 mg mL^{-1} lysozyme. Cells were crushed via pulsed sonication six times for 1 min each (with 1 min intervals between sonications) on ice and then centrifuged at 50000*g* for 60 min at 4 °C. The supernatant fractions were applied to a glutathione-Sepharose 4B column (GE Healthcare). The column was then washed with buffer B, and protein fractions were eluted with 10 mM reduced glutathione in 50 mM Tris-HCl (pH 8.0). Protein fractions were pooled and applied to a Superdex 200 10/300 GL column (GE Healthcare) equilibrated with 50 mM Tris-HCl (pH 8.0) buffer containing 150 mM NaCl. The desired eluates (identified by monitoring at 280 nm) were collected and concentrated with Amicon Ultra Centrifugal Filters (Millipore). Purified proteins were immediately frozen in liquid nitrogen and stored at −80 °C until they were used. Purified GST-RR was more than 97% homogeneous as determined by SDS−PAGE followed by staining with Coomassie Brilliant Blue. Protein concentrations were determined using the bicinchoninic acid assay with bovine serum albumin as a standard (Sunrise Absorbance Reader, TECAN).

Optical Absorption Spectroscopy. Optical absorption spectral data were obtained using an HP 8453 UV−vis spectrophotometer (Agilent Technologies, Santa Clara, CA) at 20 °C under aerobic conditions as previously described.[14] Anaerobic spectral experiments were conducted on a DeNovix DS-11 spectrophotometer in a gastight plastic box (Sigma-Aldrich, Schnelldorf, Germany) with 99.998% Ar (O_2 concentrations of <3 ppm). To ensure that the solution was maintained at an appropriate temperature (20 °C), the reaction mixture was incubated for 5 min prior to spectroscopic measurement. The Fe(II) complex was prepared in N_2-saturated buffer [50 mM Tris-HCl (pH 8.0)].

Femtosecond Spectroscopy. Ultrafast pump−probe spectroscopy with pump pulses centered at 570 nm and continuum broadband probe pulses was performed using a 500 Hz repetition rate setup as described previously.[30] Samples were prepared in gastight 1 mm optical path-length cells in 20 mM Tris (pH 8.0) with a heme concentration of 40 μM for CO experiments or 50 μM for O_2 experiments. The CO complex was prepared by exposing dithionite-reduced degassed *Af*GcHK to 1 atm of CO. For some experiments, an equimolar quantity of a degassed RR solution was also added. The O_2 complex was prepared by reducing the degassed protein with a minimal amount of dithionite and subsequently exposing it to air. This complex has a very low autoxidation rate,[14] making it amenable to characterization and experimental study.

Kinetic Analysis of *Af*GcHK Autophosphorylation. The autophosphorylation activity of *Af*GcHK was assayed under various conditions. Unless stated otherwise, the experiments were conducted at 20 °C in a reaction mixture containing 10 μM *Af*GcHK, 50 mM Tris-HCl (pH 8.0), 50 mM KCl, and 5 mM $MgCl_2$. The reaction mixture was preincubated for 5 min at 20 °C, and the reaction was initiated by adding 1 mM ATP. The reaction time was usually 60 s.

The effect of pH on *Af*GcHK autophosphorylation was tested in reaction mixtures containing various buffers. Reactions at pH 5.5, 6.0, and 6.5 were performed using 100 mM phosphate buffer (Na_2HPO_4 + NaH_2PO_4); incubations at pH 7.0, 7.5, 8.0, 8.5, and 9.0 were performed in 100 mM Tris buffer (Tris-HCl), and incubations at pH 9.5 and 10.0 were performed using 100 mM glycine buffer. The *Af*GcHK autophosphorylation assay was also performed in 50 mM NaOH (pH 12.7) and 100 mM NaOH (pH 13.0) with no buffer.

The time course of the autophosphorylation reaction catalyzed by WT and His99Ala *Af*GcHK was assayed at 20 °C in a reaction mixture containing 10 μM *Af*GcHK (WT or His99Ala), 50 mM Tris-HCl (pH 8.0), 50 mM KCl, and 5 mM $MgCl_2$. The reaction mixture was preincubated for 5 min, and then the reaction was initiated by adding 1 mM ATP at 20 °C. The state of the reaction was determined at the following time points after its initiation: 0, 0.5, 1, 2, 5, 10, 15, 20, 30, 40, 50, 60, and 180 min.

To estimate the kinetic parameters of the autophosphorylation of *Af*GcHK, a reaction mixture containing 10 μM *Af*GcHK, 5−5000 μM ATP, 50 mM Tris-HCl (pH 8.0), 50 mM KCl, and 5 mM $MgCl_2$ in a total volume of 100 μL was used. The reaction was started by the addition of ATP. The product of the autophosphorylation reaction was the His^{183}-phosphorylated form of *Af*GcHK, i.e., P-*Af*GcHK, and its rate of formation was determined by Phos-tag electrophoresis (see below). On the basis of the previously determined (see the preceding paragraph) time course for the autophosphorylation reaction catalyzed by WT *Af*GcHK, the amount of reaction product formed per minute over the first minute of the reaction was taken to be equivalent to the initial velocity of the autophosphorylation. Therefore, the reaction mixtures for determination of kinetic parameters were incubated at 20 °C for 30 s; the reaction during this period was assumed to proceed under initial velocity conditions because of the reaction's linearity over the first 1 min. The *Af*GcHK autophosphorylation reaction is a pseudobisubstrate process (the two substrates being ATP and the enzyme itself). However, the kinetic study focused on the apparent kinetics observed when the concentration of the enzyme is invariant while that of ATP is varied. Kinetic constants were determined by nonlinear least-squares regression using the Michaelis−Menten equation. The results obtained in this way were consistent with those obtained from a Lineweaver−Burk plot (Figure S1). At least three replicate experiments were performed for each set of reaction conditions, and the results obtained for each replicate performed under a given set of conditions were usually within 10% of those for the other replicates. The standard deviations over all experimental replicates performed under each set of experimental conditions are reported in the figures and tables.

DOI: 10.1021/acs.biochem.5b00517
Biochemistry 2015, 54, 5017−5029

The effects of the sensor domain's heme iron as well as its redox and coordination state on the Michaelis−Menten kinetics of the autophosphorylation reaction were investigated by varying the configuration of the sensor domain heme. The sensor domain of the isolated protein was in the Fe(III)-OH^- state. The heme Fe(II) species were prepared by placing a 20 μM solution of the Fe(III)-OH^- protein in a quartz cuvette and reducing it using 10 mM sodium dithionite. Fe(II)-CO complexes were then prepared by gently bubbling gaseous carbon monoxide (Linde, Wiesbaden, Germany) through the cuvette for 15 min. No spectral changes indicative of heme oxidation over time were detected in the spectral recordings. Sodium dithionite, which was used to reduce the Fe(III) complex, was kept in the solution throughout the experiments with the Fe(II) and Fe(II)-CO complexes to prevent Fe(II)-O_2 complex formation. Separate experiments demonstrated that the presence of sodium dithionite did not affect the measured kinetic parameters. The Fe(II)-O_2 complex was prepared by removing sodium dithionite and exposing the Fe(II) species to air for 10 min. After the kinetic experiments, we characterized the samples by UV−vis spectroscopy to verify that the heme iron species remained in the Fe(II)-O_2 form. These studies revealed no evidence of heme iron autoxidation. The Fe(III)-CN^- and Fe(III)-imidazole forms of *Af*GcHK were produced by mixing a 20 μM solution of the Fe(III)-OH^- protein with 0.1 M KCN and 0.1 M imidazole, respectively. The KCN was used in 100 mM Tris buffer (pH 8.0), and the solution's pH was monitored. Heme-free experiments were performed using the His99Ala *Af*GcHK mutant instead of the WT protein.

The effect of the RR on *Af*GcHK autophosphorylation was tested in reaction mixtures containing 10 μM GST-RR and no $MgCl_2$. The lack of Mg^{2+} was necessary to suppress the phosphotransfer reaction to GST-RR, which competes with the autophosphorylation of *Af*GcHK. To investigate the effect of the RR on the autophosphorylation reaction in the presence of 5 mM Mg^{2+}, experiments were conducted using a mutated RR variant (10 μM Asp52/169Ala GST-RR). The mutant cannot undergo the phosphotransfer reaction because it lacks the necessary active aspartic acid residues.

The effects of divalent metal ions on *Af*GcHK autophosphorylation were investigated using reaction mixtures containing solutions of different metal salts instead of $MgCl_2$. Specifically, the $MgCl_2$ was replaced with 5 mM $MnCl_2$, 5 mM $CaCl_2$, 5 mM $CoCl_2$, 5 mM $NiCl_2$, 5 mM $ZnSO_4$, or 5 mM $CdCl_2$ as appropriate. To assess the enzyme's activity in the absence of divalent metal cations, reactions were performed with no added metal salt; these reaction mixtures were analyzed by atomic absorption spectroscopy (see below) to verify that they contained no divalent metal ions.

Identification of the P-*Af*GcHK by Phos-tag Electrophoresis. At the designated times, the *Af*GcHK autophosphorylation assay reaction was terminated by adding 100 μL aliquots of termination buffer [125 mM Tris-HCl (pH 6.8), 4% SDS, 10% 2-mercaptoethanol, 20% glycerol, and 0.004% bromophenol blue]. Samples of the quenched reaction mixtures were then loaded on a 10% SDS−polyacrylamide gel containing 75 μM Phos-tag acrylamide and 0.2 mM $MnCl_2$. Each lane was loaded with a quantity of quenched reaction mixture containing 0.5 μg of *Af*GcHK. Phosphorylated proteins in the sample interacted with the Phos-tag manganese complex in the gel, reducing their mobility relative to those of phosphate-free proteins.[14,24,31] After electrophoresis, the proteins were visualized by staining with Coomassie Brilliant Blue R350 and the stained gels were imaged using a Scanjet G3010 (HP) scanner. The protein loadings were then quantified by analyzing the scanned images using ImageJ.

Atomic Absorption Spectroscopy. Reference measurements of magnesium, manganese, and calcium concentrations were acquired using an AAS 3 (Zeiss, Jena, Germany) atomic absorption spectrometer with a flame atomization unit. The spectrometer was operated using predefined optimal settings. Varian Mn, Mg, and Ca hollow cathode lamps were operated at 279.5, 285.2, and 422.7 nm, respectively, with 0.2, 0.5, and 0.5 nm spectral bandpasses, respectively. A lamp current of 5 mA was used in all cases. Atomization was performed with an air−acetylene flame for Mn and Mg or a nitrous oxide−acetylene flame for Ca. The concentration of manganese was determined without adding any chemical agents. To suppress common interference during magnesium determination, a small amount of strontium nitrate (releasing agent) was added to all samples at a final concentration of 1000 mg L^{-1}. To avoid calcium ionization during its measurement, a small amount of potassium chloride was added to all samples at a final concentration of 3000 mg L^{-1}. All reagents used were of analytical reagent grade or higher purity. Deionized water (<0.1 mS cm^{-1}, Milli-QPLUS, Millipore) was used to prepare all solutions. Working standards were prepared by diluting standard 1.000 g L^{-1} stock solutions of Mn^{2+}, Mg^{2+}, and Ca^{2+} (Merck).

RESULTS

Optimization of the Autophosphorylation Activity of *Af*GcHK in Its Native Form. Purified preparations of *Af*GcHK were phosphorylated under conditions typical for histidine kinases with ATP, KCl, and $MgCl_2$ after incubations at 20 °C for 0.5−180 min, as previously reported.[14,32] Using UV−vis spectroscopy, we investigated the previous suggestion that the heme iron in the native protein obtained after purification forms a six-coordinate low-spin Fe(III) complex with an axial hydroxyl ligand on the heme-distal side (data not shown).[14] To further characterize the autophosphorylation of the Fe(III)-OH^--bound *Af*GcHK in its native form, its kinetics were examined.

The autophosphorylation reaction catalyzed by the Fe(III)-OH^--bound *Af*GcHK is a pseudobisubstrate reaction with the first substrate being ATP and the second the enzyme itself. The initial rate of autophosphorylation was determined at various *Af*GcHK concentrations and found to increase linearly with enzyme concentration (data not shown). The apparent Michaelis constant (K_m) with respect to *Af*GcHK could not be evaluated because the enzyme is both substrate and catalyst, and the catalyst concentration must be held constant to obtain a Michaelis constant with respect to a substrate. Therefore, kinetic analyses were performed only with respect to ATP, keeping the enzyme concentration constant at 10 μM. The time course of the autophosphorylation reaction catalyzed by *Af*GcHK revealed that its progress was linear during at least the first minute (Figure 1). That is to say, the amount of reaction product (the His^{183}-phosphorylated form of *Af*GcHK, henceforth termed P-*Af*GcHK) formed per minute during the first minute of the reaction was equivalent to the initial velocity of the kinase reaction. The initial velocities of autophosphorylation were measured at various ATP concentrations (0−1000 μM) at pH 8.0 in the presence of 50 mM K^+ and 5 mM Mg^{2+} (Figure 2). The reaction follows Michaelis−Menten kinetics with an apparent K_m^{ATP} value of 18.9 ± 2.3 μM and an maximal apparent enzyme velocity with respect to ATP (V_{max}^{ATP}) of

DOI: 10.1021/acs.biochem.5b00517
Biochemistry 2015, 54, 5017−5029

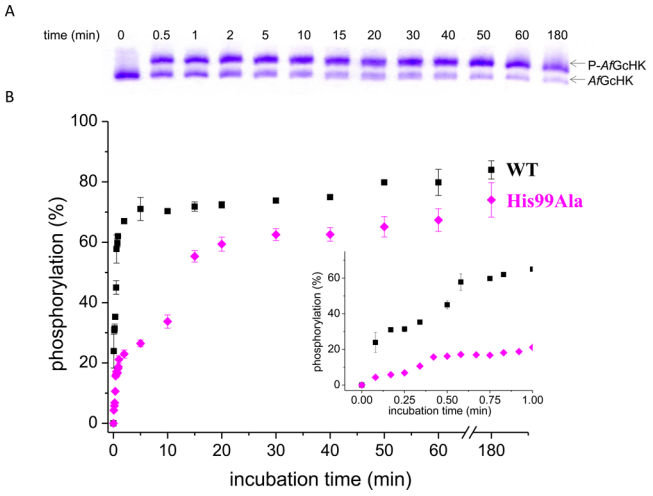

Figure 1. Time course of the histidine kinase reactions catalyzed by the WT *Af*GcHK [in its Fe(III)-OH^- form] and the His99Ala mutant of *Af*GcHK. (A) Phos-tag SDS−PAGE gel patterns demonstrating separation of *Af*GcHK and P-*Af*GcHK formed by WT *Af*GcHK at different time periods and (B) a graphical representation of the results: WT *Af*GcHK (■) and His99Ala (pink diamonds). In each run, a reaction mixture containing 10 μM *Af*GcHK (WT or His99Ala), 1 mM ATP, 50 mM Tris-HCl (pH 8.0), 50 mM KCl, and 5 mM $MgCl_2$ in a total volume of 100 μL was incubated for various time periods (for further details, see Experimental Procedures). The inset shows the expansion of initial time points of the time course plot.

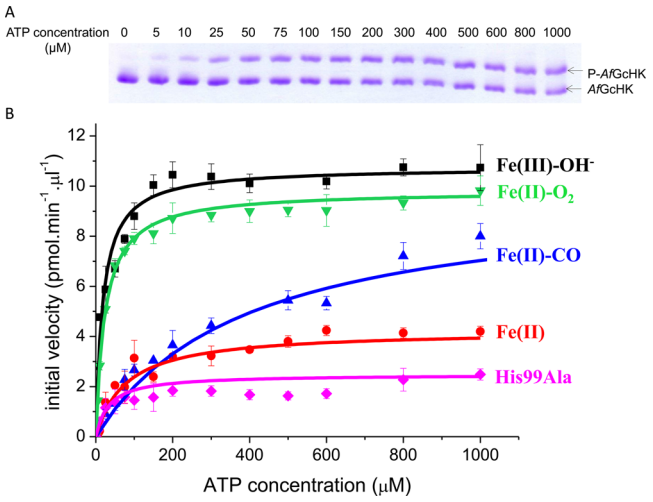

Figure 2. Effect of the heme iron redox states, heme iron ligand states, and the presence of heme iron in the sensor domain on the Michaelis−Menten kinetics of the autophosphorylation reaction catalyzed by WT *Af*GcHK. (A) Phos-tag SDS−PAGE gel patterns demonstrating separation of *Af*GcHK and P-*Af*GcHK formed by Fe(II)-O_2-bound *Af*GcHK at different ATP concentrations and (B) graphical representation of results for each of the different *Af*GcHK forms: Fe(III)-OH^- (native form, black line and squares), Fe(II)-O_2 (green line and triangles), Fe(II)-CO (blue line and triangles), Fe(II) (red line and circles), and heme-free form (His99Ala) (pink line and diamonds). In each run, a reaction mixture containing 10 μM *Af*GcHK, 0−1000 μM ATP, 50 mM Tris-HCl (pH 8.0), 50 mM KCl, and 5 mM $MgCl_2$ in a total volume of 100 μL was incubated for 30 s (for further details, see Experimental Procedures).

10.8 ± 0.3 pmol of P-*Af*GcHK min^{-1} μL^{-1}. The k_{cat} and k_{cat}/K_m^{ATP} values were determined to be 1.1 min^{-1} and 1000 M^{-1} s^{-1}, respectively (Table 1 and Figure S1).

Table 1. Effect of the Heme Iron Oxidation State, Ligand Coordination in the Sensor Domain, and the Presence of RRs (WT and Asp52/169Ala) on the Kinetic Parameters of the Autophosphorylation Reaction Catalyzed by *Af*GcHK

heme iron state in the sensor domain of *Af*GcHK or the presence of RR	K_m^{ATP} (μM)	V_{max}^{ATP} (pmol of P-*Af*GcHK min^{-1} μL^{-1})	k_{cat} (min^{-1})	k_{cat}/K_m^{ATP} (M^{-1} s^{-1})
Fe(III)-OH^- (WT, native form)	18.9 ± 2.3	10.8 ± 0.3	1.1	1000
Fe(III)-CN^-	35.4 ± 9.7	11.8 ± 0.6	1.2	600
Fe(III)-imidazole	23.8 ± 4.1	11.2 ± 0.3	1.1	800
Fe(II)-O_2	23.0 ± 1.3	9.6 ± 0.1	1.0	700
Fe(II)-CO	357.0 ± 28.0	10.4 ± 0.3	1.0	50
Fe(II)	78.0 ± 4.7	4.2 ± 0.2	0.4	90
no heme (His99Ala *Af*GcHK)	33.6 ± 1.7	2.5 ± 0.1	0.3	120
Fe(III)-OH^- and Asp52/169Ala RR	47.7 ± 1.4	10.0 ± 0.3	1.0	300
Fe(III)-OH^- and WT RR (in the absence of Mg^{2+})	152.0 ± 10.6	1.8 ± 0.2	0.16	20

Effect of pH on the Autophosphorylation Reaction Catalyzed by the Fe(III)-OH^--Bound *Af*GcHK. The efficiency of the autophosphorylation of the Fe(III)-OH^--bound *Af*GcHK was examined by measuring the amount of P-*Af*GcHK formed over an experimental period of 1 min using reaction mixtures containing 50 mM K^+ and 5 mM Mg^{2+} at pH values ranging from 5.5 to 13 (Figure 3). The enzyme was

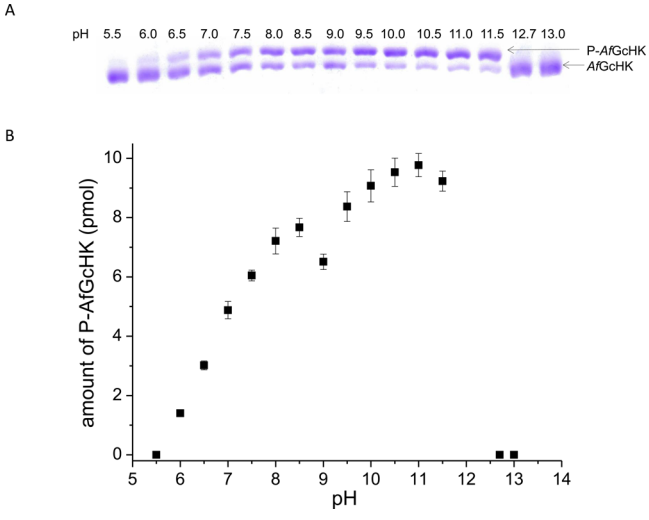

Figure 3. Effect of pH on the autophosphorylation reaction catalyzed by WT *Af*GcHK [in its Fe(III)-OH^- form]. (A) Phos-tag SDS−PAGE gel patterns demonstrating separation of *Af*GcHK and P-*Af*GcHK formed by Fe(III)-OH^--bound *Af*GcHK at different pH values and (B) a graphical representation of the results. In each run, a reaction mixture containing 10 μM *Af*GcHK, 1 mM ATP, 50 mM KCl, 5 mM $MgCl_2$, and an appropriate pH buffer (100 mM) in a total volume of 100 μL was incubated for 60 s (for further details, see Experimental Procedures). Note that the discontinuity at pH 9.0 is reproducible and may be due to a change in the axial ligand from OH^- to Tyr-O^-.

inactive below pH 5.5 or above pH 12.7 but exhibited discernible activity at between pH 6.0 and 11.5. Within this range, its activity exhibited an asymmetric bell-shaped dependence upon pH. Its optimal pH was around 11.0; the rate of autophosphorylation at pH 7.0 was around half that observed at

DOI: 10.1021/acs.biochem.5b00517
Biochemistry 2015, 54, 5017−5029

the optimal pH, while at pH 8.0, it was around 75% of the optimal rate. We conducted our subsequent experiments at pH 8.0 because these mildly alkaline conditions are optimal for preserving the conformation and stability of *Af*GcHK.[14] Moreover, pH 8.0 is more physiologically relevant than pH 11.0.

_Af_GcHK Retains Catalytic Activity When the Native Hydroxyl Ligand of the Sensor Domain Heme Iron Is Replaced with Cyanide or Imidazole (Figure 4). As mentioned previously, the six-coordinate low-spin Fe(III) complex with an axial hydroxyl ligand at the heme-distal side of *Af*GcHK, Fe(III)-OH^-, is fully enzymatically active (Figure 2 and Table 1). Experiments were performed to determine how the coordination of alternative external ligands to the Fe(III) complex affected the functional domain's catalytic activity (Table 1 and Figure 4). Both the Fe(III)-CN^- and Fe(III)-imidazole forms of *Af*GcHK were enzymatically active with kinetic parameters that were very similar to those for the Fe(III)-OH^- complex (Table 1 and Figure 4).

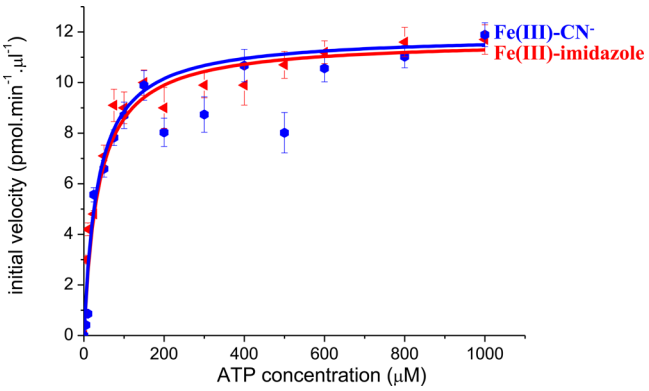

Figure 4. Effects of binding of cyanide and imidazole to the heme iron in the sensor domain on the Michaelis–Menten kinetics of the autophosphorylation reaction catalyzed by Fe(III)-bound *Af*GcHK: Fe(III)-CN^- (blue line and hexagons) and Fe(III)-imidazole (red line and triangles). In each run, a reaction mixture containing 10 μM *Af*GcHK, 0–1000 μM ATP, 50 mM Tris-HCl (pH 8.0), 50 mM KCl, and 5 mM $MgCl_2$ in a total volume of 100 μL was incubated for 30 s (for further details, see Experimental Procedures).

The Heme Fe(II) Complex of _Af_GcHK Exhibits Low Activity but Is Activated by the Coordination of CO or O_2. While the six-coordinate low-spin Fe(III) complexes [Fe(III)-OH^-, Fe(III)-CN^-, and Fe(III)-imidazole] of *Af*GcHK are fully catalytically active (Figures 2 and 4 and Table 1), the five-coordinate high-spin Fe(II) complex of the same enzyme was significantly less active (Figure 2 and Table 1). While a detailed kinetic analysis of the reaction catalyzed by the Fe(II) complex of *Af*GcHK revealed that it followed Michaelis–Menten kinetics (Figure 2), its K_m^{ATP} value (78 μM) was more than 4 times greater than that for the Fe(III) complexes of *Af*GcHK, and its V_{max}^{ATP} value (4.2 pmol of P-*Af*GcHK min^{-1} μL^{-1}) was around half that for the Fe(III) complexes. The latter of these findings shows that the low activity of the five-coordinate high-spin Fe(II) complex is due to its low basal autophosphorylation activity compared to those of the Fe(III) complexes of *Af*GcHK. The effect of reducing the sensor domain heme iron on the autophosphorylation reaction is similar to that of removing the heme iron altogether, as discussed below (Figure 2 and Table 1).

When the Fe(II) complex of *Af*GcHK was exposed to either O_2 or CO, its catalytic activity was dramatically enhanced. The enzyme kinetics of the Fe(II)-O_2 complex closely resemble those of the Fe(III)-OH^- complex (Figure 2). Likewise, the kinetic parameters (K_m^{ATP} and V_{max}^{ATP}) of the Fe(III)-OH^- and Fe(II)-O_2 complexes are also very similar (Table 1).

The coordination of CO to the Fe(II) complex had remarkable effects: the K_m^{ATP} value of the resulting Fe(II)-CO complex was ~20 times higher than that of the parent Fe(II) complex, and its V_{max}^{ATP} value was similar to those for the Fe(III)-OH^- and Fe(II)-O_2 complexes. The strong increase in K_m^{ATP} caused by the coordination of CO suggests a dramatic reduction in the enzyme's affinity for ATP (Figure 2 and Table 1).

The Heme-Free Enzyme Has Low Activity. Two different strategies were used to study the effect of the heme's presence in the sensor domain on the autophosphorylation activity of *Af*GcHK. Experiments were performed using either (i) the apo form of WT *Af*GcHK or (ii) His99Ala *Af*GcHK. It was difficult to obtain pure samples of the apo WT *Af*GcHK protein because the prepared material always contained some traces of heme (data not shown), which hampered the interpretation of the kinetic analyses. Consequently, the second approach using the His99Ala mutant was adopted. It has been shown that the histidine residue at position 99 is the proximal axial ligand of the heme iron;[14] when this ligand is replaced with alanine, the protein loses its heme binding ability. This makes it straightforward to prepare the His99Ala mutant in a pure heme-free form.

Figure 2 shows the effect of the absence of the sensor domain heme on the Michaelis–Menten kinetics of the autophosphorylation reaction catalyzed by the heme-free apo form of *Af*GcHK His99Ala. The results obtained indicate that the heme's presence was essential for effective autophosphorylation by the functional domain. The V_{max}^{ATP} value for the autophosphorylation of *Af*GcHK without the sensor domain heme (His99Ala) was approximately 4 times lower than that of WT (Table 1). The absence of the heme in the sensor domain also reduced the mutant apo form's affinity for ATP: its K_m^{ATP} value was approximately twice that of the heme-containing WT *Af*GcHK enzyme (Table 1).

To determine whether coordination of the heme iron in the sensor domain was required for the autophosphorylation of the functional domain of *Af*GcHK, it was necessary to prove that the His99Ala mutation does not hinder the correct folding of the kinase domain. The time course of the autophosphorylation of the His99Ala mutant was monitored (Figure 1B) for that purpose.

The time course of the His99Ala autophosphorylation (Figure 1B) differed from that for WT *Af*GcHK. The reaction of His99Ala was significantly slower than that of the WT: the autophosphorylation of the WT went to completion within 5 min, but that of His99Ala took >60 min. Consequently, experiments conducted over longer periods of time (>60 min) would misleadingly suggest that the WT and His99Ala mutant have very similar activity. This may be why Kitanishi et al.[14] suggested that the presence of the heme iron in the sensor domain does not affect the activity of the functional domain; they examined the outcome of the autophosphorylation reaction only after an extended incubation period and did not investigate the enzyme's kinetics. The results indicate that the His99Ala mutant's functional domain is folded correctly and capable of autophosphorylation.

RR Binding Reduces the Affinity of _Af_GcHK for ATP. An abortive RR double mutant (Asp52/169Ala) in which the aspartate residues of the phosphorylation sites were replaced

DOI: 10.1021/acs.biochem.5b00517
Biochemistry 2015, 54, 5017–5029

with alanine residues that cannot be phosphorylated was used to investigate the effect of the RR on *Af*GcHK autophosphorylation. It was necessary to use the double mutant because the WT RR induces a phosphotransfer reaction from phosphorylated *Af*GcHK that interferes with the autophosphorylation of *Af*GcHK. The K_m^{ATP} value (47.7 μM) for autophosphorylation of *Af*GcHK in the presence of Asp52/169Ala RR was 2.5-fold higher than that in the absence of RR [18.9 μM (Table 1 and Figure 5)]. This finding suggests that the presence of the RR

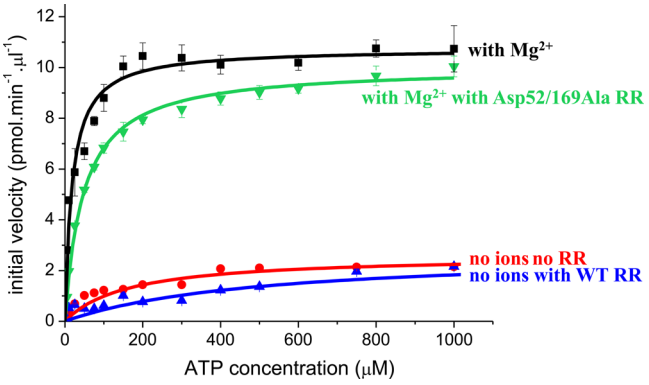

Figure 5. Effects of WT and Asp52/169Ala RR on the autophosphorylation of native *Af*GcHK. Note that WT RR in the presence of Mg^{2+} also catalyzes its autophosphorylation reaction, which competes with the studied process (autophosphorylation of *Af*GcHK): in the presence of Mg^{2+} and Asp52/169Ala RR (green line and triangles), in the presence of Mg^{2+} and in the absence of Asp52/169Ala RR (black line and squares), in the absence of both Mg^{2+} and RR (red line and circles), and in the absence of Mg^{2+} and in the presence of RR (blue line and triangles). In each run, a reaction mixture containing 10 μM *Af*GcHK and 0 or 10 μM RR (WT or Asp52/169Ala), 5−1000 μM ATP, 50 mM Tris-HCl (pH 8.0), 50 mM KCl, and 0 or 5 mM $MgCl_2$ in a total volume of 100 μL was incubated for 30 s (for further details, see Experimental Procedures).

mutant protein significantly reduces the affinity of *Af*GcHK for ATP. The RR-binding site of *Af*GcHK is probably located close to the ATP-binding site such that the binding of the RR interferes with that of ATP. Interestingly, the V_{max}^{ATP} value of *Af*GcHK was not significantly affected by the presence of the RR mutant (Table 1).

As an alternative way of eliminating the competing phosphotransfer reaction to the Asp52 and Asp169 residues of the RR, we studied the effect of the wild-type RR protein on the autophosphorylation activity of *Af*GcHK in the absence of Mg^{2+} ions. The WT RR protein did not affect the V_{max}^{ATP} value (1.8−2.2 pmol of P-*Af*GcHK min^{-1} μL^{-1}) associated with the very low basal autophosphorylation activity of *Af*GcHK under these conditions (Table 2), but the K_m^{ATP} value for *Af*GcHK in the presence of WT RR (152.0 μM) was 2.7 times greater than that in the absence of RR (55.9 μM) under the same conditions (Figure 5 and Tables 1 and 2). These results are consistent with those obtained in the experiments using the double mutant: both suggest that the presence of the RR protein significantly reduces the affinity of *Af*GcHK for ATP because the RR protein-binding site is probably situated close to the ATP-binding site.

Characterization of Ultrafast CO and O_2 Dissociation and Binding Kinetics. We examined the kinetics of CO and O_2 binding to and dissociation from the heme iron of *Af*GcHK on the femto- to nanosecond time scales using transient

Table 2. Effect of Divalent Metal Ions (Mg^{2+}, Mn^{2+}, Ca^{2+}, Co^{2+}, Ni^{2+}, Zn^{2+}, and Cd^{2+}) on the Kinetic Parameters of the Autophosphorylation Reaction Catalyzed by Fe(III)-Bound *Af*GcHK

ion for incubation of Fe(III)-bound *Af*GcHK	K_m^{ATP} (μM)	V_{max}^{ATP} (pmol of P-*Af*GcHK min^{-1} μL^{-1})	k_{cat} (min^{-1})	k_{cat}/K_m^{ATP} (M^{-1} s^{-1})
Mg^{2+}	18.9 ± 2.3	10.8 ± 0.3	1.1	1000
Mn^{2+}	93.2 ± 9.5	13.1 ± 0.3	1.3	233
Ca^{2+}	403.9 ± 105.4	6.9 ± 0.8	0.7	30
Co^{2+}	no reaction			
Ni^{2+}	no reaction			
Zn^{2+}	no reaction			
Cd^{2+}	no reaction			
no ions	55.9 ± 4.1	2.2 ± 0.1	0.2	60

absorption spectroscopy. The Fe(II)-CO and Fe(II)-O_2 forms of *Af*GcHK represent two extremes of catalytic efficiency, with the former complex's affinity for ATP being more than 1 order of magnitude lower than the latter's (Table 1). Selected transient spectra in the Soret region for the dissociation from the WT Fe(II)-CO complex are shown in Figure 6A. The difference spectra show the red shift that is typical for transitions from a six-coordinate state to a five-coordinate one. After spectral relaxations due to photophysical processes (not shown), which mainly occur over time scales of up to a few picoseconds,[33] the spectra become almost identical in shape but with diminished amplitudes, reflecting substantial geminate heme-CO recombination on the pico- to nanosecond time scale. A global analysis assuming multiexponential decay revealed rebinding phases of 170 ps (24%), 1.5 ns (49%), and >4 ns (27%). Such multiphasic rebinding behavior is observed in many heme proteins[30,34−39] and may reflect a process whereby CO samples a distribution of heme environments prior to rebinding, in competition with escape from the heme pocket.

This kinetic behavior is markedly different from that observed for myoglobin, mammalian hemoglobin, and the globin-coupled oxygen sensor YddV (unpublished results), where virtually no geminate rebinding occurs. However, it is qualitatively similar to that of truncated bacterial hemoglobins.[37,38]

Analyses of the kinetics of CO dissociation can be used to sensitively probe the heme environment, as demonstrated by experiments on genetically modified proteins.[36,38−41] This is also the case for *Af*GcHK (Figure S2). The inset of Figure 6A shows that in contrast to the results obtained for other enzymes, the kinetics of CO rebinding are not affected by the presence of the RR protein. This suggests that whereas the coordination state of the heme domain affects the catalytic efficiency of the enzymatic domain by modulating its ATP affinity, there is no significant reverse effect. In general terms, this finding is consistent with the observation that the CO rebinding kinetics of the heme domain of *Ec* Dos do not depend on the catalytic domain's presence.[42]

Excitation of the Fe(II)-O_2 complex of *Af*GcHK yielded a signal that was far weaker than the CO dissociation signal and featured a small red-shift that evolved on the time scale of hundreds of femtoseconds to a few picoseconds (Figure 6B). These findings are similar to those achieved for other sensor complexes and presumably reflect heme photophysics, including cooling of the heme. The quantum yield (QY) of

DOI: 10.1021/acs.biochem.5b00517
Biochemistry 2015, 54, 5017−5029

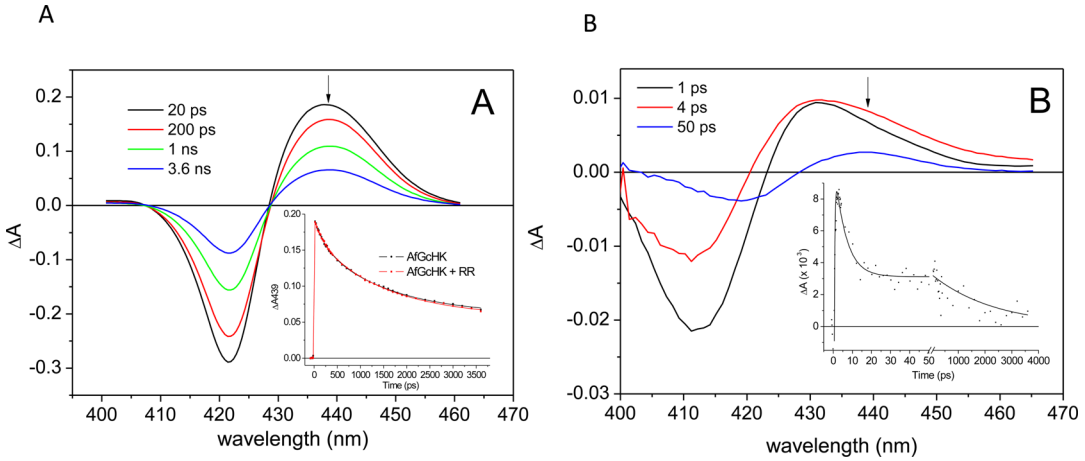

Figure 6. Selected transient spectra of WT *Af*GcHK upon (A) CO and (B) O_2 dissociation. The insets show kinetics at (A) 439 and (B) 440 nm, for panel A in the presence and absence of stoichiometric amounts of the response regulator. Note the difference in signal amplitude in the two panels.

dissociated O_2 after these phases can be estimated by comparing the signal's amplitude to that of the steady-state difference spectrum and using MbCO dissociation (100% QY) under the same experimental conditions as a reference.[43,44] In this way, the QY at 50 ps was estimated to be ~1.8%. This very low value (for comparative purposes, the QY of MbO_2 is ~30%) is similar to those reported for other O_2 sensor and heme proteins (~5% for FixL-O_2[43] and ~1% for HbO from *M. tuberculosis*[38]). The effective O_2 escape yield was lower still because the majority of the dissociated O_2 rebound on a time scale of a few nanoseconds (Figure 6B, inset). Thus, *Af*GcHK appears to act as a highly efficient O_2 trap.

Effects of Divalent Metal Cations on *Af*GcHK Autophosphorylation. We tested the effect of several divalent metal cations (Mg^{2+}, Mn^{2+}, Ca^{2+}, Co^{2+}, Ni^{2+}, Zn^{2+}, and Cd^{2+}) on the autophosphorylation activity of *Af*GcHK (Figure 7 and Table 2). It was confirmed by atomic absorption spectroscopy that there were no traces of the aforementioned divalent ions in the isolated *Af*GcHK sample (Figure S3).

Of the divalent cations investigated, Mg^{2+} ions were by far the most effective at stimulating autophosphorylation in terms of k_{cat}/K_m^{ATP} values (Figure 7 and Table 2). Moreover, the K_m^{ATP} value (93.2 μM) in the presence of Mn^{2+} was approximately 5 times higher than that (18.9 μM) in the presence of Mg^{2+}. The V_{max}^{ATP} value (13.1 pmol of P-*Af*GcHK min^{-1} μL^{-1}) in the presence of Mn^{2+} was slightly higher than that (10.8 pmol of P-*Af*GcHK min^{-1} μL^{-1}) in the presence of Mg^{2+}. Considering that both Mg^{2+} and Mn^{2+} form the metal-ATP complex, these results suggest that the enzyme's affinity for the Mn^{2+}-ATP complex and the orientation of ATP in its active site are different from those of the Mg^{2+}-ATP complex.

It was also found that Ca^{2+} ions can serve as divalent ion cofactors that facilitate the autophosphorylation of *Af*GcHK. However, they are less effective in this role than Mg^{2+}, which is reflected by the significantly higher K_m^{ATP} value (403.9 μM) observed in the presence of Ca^{2+} compared to that with either Mg^{2+} or Mn^{2+} (Figure 7 and Table 2).

It should be emphasized that while the V_{max}^{ATP} value observed in the presence of Mg^{2+} ions (10.8 pmol of P-*Af*GcHK min^{-1} μL^{-1}) is >4 times greater than that observed in the absence of divalent metal ions (2.2 pmol of P-*Af*GcHK min^{-1} μL^{-1}), the enzyme retains a low basal level of activity even when no divalent metal ion is present. It is therefore interesting that the presence of Co^{2+}, Ni^{2+}, Zn^{2+}, or Cd^{2+}

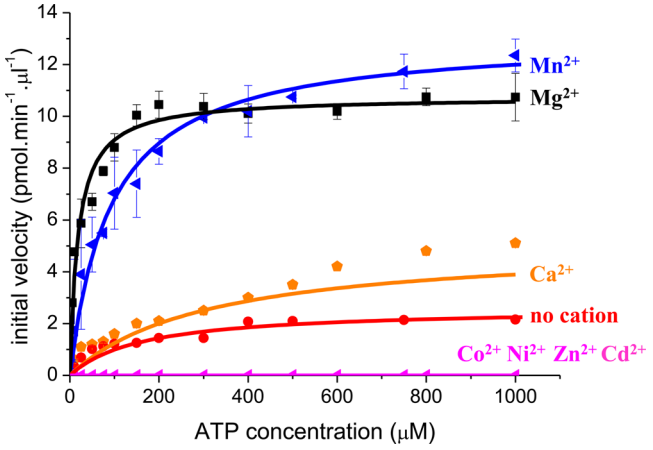

Figure 7. Effect of divalent metal ions on the autophosphorylation reaction catalyzed by the native form of *Af*GcHK: Mg^{2+} (black line and squares), Mn^{2+} (blue line and triangles), Ca^{2+} (orange line and pentagons), Co^{2+}, Ni^{2+}, Zn^{2+}, and Cd^{2+} (pink line and triangles), and no divalent cations (red line and circles). In each run, a reaction mixture containing 10 μM *Af*GcHK, 5−1000 μM ATP, 50 mM Tris-HCl (pH 8.0), 50 mM KCl, and 0 or 5 mM $MgCl_2$, 5 mM $MnCl_2$, 5 mM $CaCl_2$, 5 mM $CoCl_2$, 5 mM $NiCl_2$, 5 mM $ZnSO_4$, or 5 mM $CdCl_2$ in a total volume of 100 μL was incubated for 30 s (for further details, see Experimental Procedures).

completely suppresses even the metal-free basal autophosphorylation activity. Presumably, these divalent metal ions cause the formation of a metal-ATP complex that is incapable of undergoing the phosphate−phosphate bond cleavage required for the autophosphorylation reaction.

DISCUSSION

The results presented herein demonstrate for the first time that the initial velocity of the autophosphorylation reaction catalyzed by the heme Fe(III)-OH^--bound form of *Af*GcHK follows Michaelis−Menten kinetics with respect to the concentration of ATP (Figure 2). Furthermore, it was found that the catalytically optimal pH value for *Af*GcHK autophosphorylation is in the alkaline region, around pH 10.0−11.0 (Figure 3). The UV−vis spectrum of the Fe(III) complex was stable over a pH range of 7.0−10.0.[14] The pK_a values for water coordinated to sperm whale myoglobin and human hemoglobin are 8.99 and 8.05, respectively, whereas

DOI: 10.1021/acs.biochem.5b00517
Biochemistry 2015, 54, 5017−5029

that of Tyr-OH is 10.9.[28] It is therefore possible that the OH^- axial ligand would be replaced by Tyr-O^- at pH >8 or >9, and this process may be linked to the catalytic enhancement observed under alkaline conditions, although it should be noted that such conditions would also affect the properties of the phosphorylatable histidine residue. The histidine kinase reaction involved in most enzymatic autophosphorylations occurs under mildly alkaline conditions.[32,45−47] For example, it was shown that CheA autophosphorylation has an optimal pH of approximately 8.4.[46] In contrast, FixL autophosphorylation is relatively insensitive to variation in pH over a wide range but has an optimum close to pH 7.5.[32]

We have previously shown that the heme Fe(III)-OH^--, Fe(II)-O_2-, and Fe(II)-CO-bound forms of *Af*GcHK are active whereas the heme Fe(II)-bound form is inactive.[14] Furthermore, it was shown that the heme-free His99Ala mutant is active but shows unusual catalytic behavior. In this work, we determined the values of kinetic parameters such as K_m^{ATP}, V_{max}^{ATP}, and k_{cat} for the catalytic autophosphorylation of *Af*GcHK under various conditions, taking into consideration the effects of the heme iron's redox and coordination states as well as the presence of the enzyme's response regulator on its catalytic behavior.

The kinetic parameters (V_{max}^{ATP} and k_{cat}) determined for the catalytic autophosphorylation of the Fe(III)-OH^-, Fe(II)-O_2, and Fe(II)-CO heme complexes of the *Af*GcHK histidine kinase were consistent with previous reports (Figures 2 and 4 and Table 1).[14] This work also showed for the first time that the heme Fe(III)-CN^-- and Fe(III)-imidazole-bound forms are also active and have kinetic parameters that differ only slightly from those for the Fe(III)-OH^- complex (Figure 4 and Table 1). The V_{max}^{ATP} and k_{cat} values of these active forms were 9.6−11.8 pmol of P-*Af*GcHK min^{-1} μL^{-1} and 1.0−1.2 min^{-1}, respectively, suggesting that all of the active complexes have similar active site structures that support optimal activity (Figure 8). In all of the enzyme's active forms, the heme iron complex exists in a six-coordinate low-spin state. On the basis of the known structures of hemoglobin and myoglobin, the heme iron in such complexes lies in the heme plane. Conversely, the inactive Fe(II) complex exists in a five-coordinate high-spin state. On the basis of the structures of the corresponding hemoglobin and myoglobin complexes, the iron cation in such species will lie outside the heme plane. This difference in the heme coordination structures of the active and inactive forms may partially explain the heme structure-dependent catalytic regulation of *Af*GcHK.

The conformational changes associated with changes in the coordination or oxidation state of the heme iron in the sensor domain could result in either substantial rearrangements of the catalytic domain or simply an unmasking of the active site. The experiments presented herein are not adequate to characterize these conformational changes in any detail. However, as mentioned above, we suggest that the activation of the functional domain is dependent on the formation of a six-coordinate low-spin heme iron complex. Very similar results have been reported for another heme-based oxygen sensor, *Ec* DOS, which forms active low-spin complexes such as heme Fe(III)-CN^-, Fe(III)-imidazole, Fe(II)-O_2, and Fe(II)-CO.[48,49] Low-spin complexes of other heme-based sensor proteins such as the Fe(II)-O_2 and Fe(II)-CO complexes of globin-coupled diguanylate cyclase (YddV) are also active.[50,51]

In contrast to their V_{max}^{ATP} and k_{cat} values, the K_m^{ATP} values of these heme-bound active forms (18.9−357 μM) varied over

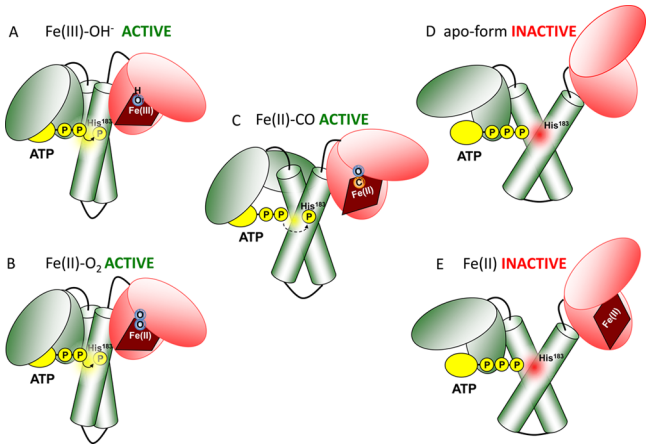

Figure 8. Schematic representation of the sensor domain's effect on the functional domain's activity for various sensor domain heme iron redox and coordination states. *Af*GcHKs with (A) Fe(III)-OH^-, (B) Fe(II)-O_2, and (C) Fe(II)-CO complexes are active in autophosphorylation, whereas (D) heme-free *Af*GcHK and (E) *Af*GcHK with Fe(II) have low activities. Presumably, the autophosphorylation reaction of dimeric *Af*GcHK would occur in a "crosswise" fashion, with a phosphate moiety being transferred from an ATP molecule bound to one subunit to the His183 residue of the other. It is also likely that the RR-binding site is close to the ATP-binding site. To avoid confusion, the figure shows autophosphorylation occurring on only one subunit of the dimeric protein.

more than 1 order of magnitude (Table 1). This suggests that the redox and/or coordination state of the heme iron in the oxygen sensing domain has profound effects on the ATP affinity of the active site in the functional domain. However, it should be remembered that all of these active forms have very similar k_{cat} values of 1.0−1.2 min^{-1}. It is noteworthy that the K_m^{ATP} value (357 μM) of the heme Fe(II)-CO complex is substantially higher than those of the Fe(III)-OH^- and Fe(II)-O_2 complexes (18.9−23.0 μM). The binding of CO to the heme Fe(II) complex in the oxygen-sensing domain presumably induces significant structural changes in the ATP-binding site that differ from those induced by alternative axial ligands such as cyanide, imidazole, and O_2. In terms of k_{cat}/K_m^{ATP}, the catalytic efficiency of the enzyme with the heme Fe(II)-O_2 complex (700 M^{-1} s^{-1}) is significantly greater than that with the heme Fe(II)-CO complex (50 M^{-1} s^{-1}) (Table 1), implying that O_2 binding and CO binding have different effects on catalytic regulation (Figure 8). Spectroscopic data on the heme Fe(II)-CO and Fe(II)-O_2 enzymes did not provide useful insights into the structure of the functional domain's active site because the spectra provided information about only the structure in the vicinity of the heme-binding site in the oxygen-sensing domain.[14] Nevertheless, the binding mode of CO differs from that of O_2 because the k_{off} and K_d values of CO among the Tyr45 mutants did not differ substantially from those for the WT enzyme even though these mutants exhibited dramatic differences in their O_2 binding. Tyr45 is believed to play an important role in binding O_2 within the Fe(II)-O_2 complex.[14] Moreover, it seems that O_2 binding occurs more rapidly than that of CO.[14]

Conversely, the data for the dissociation (and subsequent ultrafast rebinding) of CO and O_2 from the Fe(II) complexes examined in this study do provide new insights into the functional properties of the sensing domain when considered in conjunction with previously determined ligand binding and

DOI: 10.1021/acs.biochem.5b00517
Biochemistry 2015, 54, 5017−5029

dissociation data.[14] Upon dissociation, the Fe(II)-CO complex of *Af*GcHK displays a high fraction of geminate heme-CO recombination, which is unusual in hemoglobins and presumably contributes significantly to the relatively low rate of overall dissociation of CO from the protein.[14] Interestingly, qualitatively similar CO rebinding properties are observed in truncated bacterial hemoglobins[37,38] that have similar hydrophobic heme pockets featuring close-lying tyrosine and leucine residues.

The ligand dynamics of the O_2 complex are of more direct functional relevance to the enzyme's behavior *in vivo*. We found that, as for other heme-based oxygen sensors such as FixL, *Ec* DOS, and *M. tuberculosis* DosT,[52,53] the effective photodissociation yield (on the picosecond time scale) of the Fe(II)-O_2 *Af*GcHK complex was very low (1.8%, which is more than 1 order of magnitude lower than the corresponding value for Mb). On the basis of the assumption that the intrinsic thermal Fe-O_2 complex dissociation rate is similar to those of other heme proteins, we previously interpreted this behavior in terms of strain on the bound O_2, which would force its rebinding to the heme following the breaking of the heme−O_2 bond even prior to heme doming, i.e., within ∼100 fs.[43] In the case of *Af*GcHK, this strain may be induced by interactions with the proximal tyrosine residue.[14] The effective rate of dissociation is further reduced by substantial recombination on a time scale of a few nanoseconds. Overall, the *Af*GcHK heme pocket acts as a highly efficient O_2 trap, which may explain the enzyme's low O_2 dissociation rate.[14] Although *Af*GcHK is different from other O_2 sensors in that its O_2 affinity is surprisingly high and its catalytic activity is increased rather than decreased by O_2 binding,[14] the "O_2 trap" property demonstrated here is present in a variety of O_2 sensor proteins.[54] This property effectively makes the sensor a bistable switch, which helps to ensure that its reaction time is well-matched to physiologically relevant response times.

The heme-free form of *Af*GcHK, His99Ala, is relatively inactive as demonstrated by its k_{cat} value of 0.3 min^{-1} (Figure 2 and Table 1). This finding is similar to results obtained for a heme-based oxygen sensor phosphodiesterase of *Acetobacter xylinum*, *Ax*PDEA1,[55] and a heme-based oxygen sensor adenylate cyclase of *Leishmania*, HemAC-Lm;[56] in both cases, the heme-free forms had very low activities. The binding of heme to the sensor domain presumably causes significant and profound structural changes in the active site that allow the efficient functioning of these heme-based oxygen sensors (Figure 8). However, the results obtained for *Af*GcHK differ from those for heme-based oxygen sensors such as the phosphodiesterase *Ec* DOS and the diguanylate cyclase YddV from *E. coli*, whose heme-free forms have appreciable catalytic activity. It was suggested that the heme iron complexes of *Ec* DOS and YddV suppress catalysis when bound to the oxygen-sensing domain, and that O_2 binding relieves this suppression.

The addition of the abortive RR double mutant Asp52/169Ala to the heme Fe(III)-OH^- complex of *Af*GcHK significantly increased the K_m^{ATP} value of the latter protein from 18.9 to 47.7 μM without affecting its k_{cat} value (Figure 5 and Table 1). This strongly suggests that RR binds in the proximity of the enzyme's catalytic site and hampers the binding of ATP to the active site. Our finding that the presence of the RR does not influence the ligand dynamics in the sensor domain (Figure 6A, inset) is consistent with the notion that it binds specifically to the catalytic domain. Moreover, given the sensitivity of the CO binding kinetics to the details of the heme pocket's composition, this finding implies that RR binding does not induce a significant structural change in the sensor domain. Thus, whereas the heme configuration affects the functional properties of the catalytic domain, the reverse appears not to be the case.

The kinetic parameters for the active form of another histidine kinase, CheA (K_m^{ATP} = 0.26 mM; k_{cat} = 17 min^{-1}),[57] are strikingly different from those for *Af*GcHK. This is unsurprising because CheA belongs to a different family of histidine kinases. However, as shown in Table 1, the kinetic parameters determined for *Af*GcHK are quite similar to those for other heme-containing oxygen sensor histidine kinases from two-component signal transduction systems such as *Bj*FixL (K_m^{ATP} = 47 μM; k_{cat} = 0.006 min^{-1}),[58,59] DevS (K_m^{ATP} = 73 μM; k_{cat} not determined),[10] DosT (K_m^{ATP} = 39 μM; k_{cat} not determined),[10] and HpkA (K_m^{ATP} = 25 μM; k_{cat} = 0.025 min^{-1}).[60] We therefore suggest that these histidine kinases have a common molecular mechanism of action that allows them to regulate various processes in bacterial cells. Note that the k_{cat} value of the active form of *Af*GcHK is around 1 min^{-1} (Table 1). This value is comparable to those determined for an artificial light-regulated histidine kinase (0.9 min^{-1})[61] and the hemoprotein CYP1B1 (0.3−4.4 min^{-1}), both of which belong to different groups of heme-containing enzymes.[62]

The intracellular ATP concentration in bacteria is generally predicted to be between 2 and 10 mM.[63−65] Because the highest K_m^{ATP} value determined for the different *Af*GcHK complexes considered in this work was 357 μM, the k_{cat} values obtained for *Af*GcHK probably reflect its actual catalytic activity in cells (Table 1). This suggests that heme-free *Af*GcHK and the heme Fe(II) complex are less active forms whereas the heme Fe(III)-OH^-, Fe(III)-CN^-, Fe(III)-imidazole, Fe(II)-CO, and Fe(II)-O_2 complexes are active forms. Because the autoxidation rate of the heme Fe(II)-O_2 complex is very slow,[14] it is suggested that the heme Fe(II) and Fe(II)-O_2 complexes exist in equilibrium *in vivo*, that the position of this equilibrium will depend on the local O_2 concentration, and that it regulates the enzyme's catalytic activity in response to external stimuli. This is reflected in the different catalytic efficiencies of these two complexes: the k_{cat}/K_m^{ATP} values determined for the less active heme Fe(II) and the active heme Fe(II)-O_2 species were 90 and 700 M^{-1} s^{-1}, respectively (Table 1).

It was also found that Mg^{2+} and Mn^{2+} ions substantially enhanced the autophosphorylation activity of *Af*GcHK, although the presence of a divalent metal ion does not appear to be essential for the reaction (Figure 7 and Table 2). Mg^{2+} (or Mn^{2+}) is often important for phosphate-, nucleic acid-, or nucleotide-associated reactions because it can form ionic bonds with phosphate groups, which greatly facilitates their transfer.[66−68]

In contrast to our findings in the case of FixL catalysis, the most effective divalent cation was a Mn^{2+}, causing a 20-fold increase in the initial rate of autophosphorylation compared to that with Mg^{2+}.[32] Conversely, Mg^{2+} was the most effective divalent cation at enhancing the histidine kinase activity of DosT, whereas Mg^{2+} and Mn^{2+} were comparable in their ability to enhance the histidine kinase activity of DevS.[10] It should be noted that the phosphodiesterase activity of the heme-based oxygen sensor *Ec* DOS was substantially enhanced when external axial ligands such as O_2, CO, cyanide, and imidazole were bound to the heme in the presence of Mg^{2+}.[48,49] Importantly, however, the enzyme's activity was quite high

DOI: 10.1021/acs.biochem.5b00517
Biochemistry 2015, 54, 5017−5029

even in the absence of those external axial ligands when Mn^{2+} was used instead of Mg^{2+}.[1,69,70] This was taken to imply that Mn^{2+} may be bound or coordinated within the active site, and that the Mn^{2+}-bound form of *Ec* DOS without exogenous ligands mimics the Mg^{2+}-bound form with those ligands. Thus, one plausible explanation for the gas sensing function of *Ec* DOS and other heme-based oxygen sensor proteins is that binding of O_2 (or NO/CO) to the heme enhances the active site's affinity for Mg^{2+} and/or creates a Mg^{2+} coordination structure that is optimal for efficient phosphodiesterase catalysis.[69,70] However, the results presented herein for *Af*GcHK raise another possibility: the affinity of ATP for the active site or the orientation of the metal-ATP complex in the active site can be modulated by the binding of oxygen to the heme. This is supported by the observation that the K_m^{ATP} values measured for *Af*GcHK varied strongly with the heme's oxidation and coordination states, the presence of the RR, and the binding of divalent cations other than Mg^{2+} (Table 2).

We also tested the effects of other divalent metal ions such as Ca^{2+}, Co^{2+}, Ni^{2+}, Zn^{2+}, and Cd^{2+}. While Ca^{2+} ions can partly reproduce the effects of Mg^{2+} and Mn^{2+} on the *Af*GcHK autophosphorylation reaction, the other tested ions totally inhibit the process. The deviation from the Michaelis−Menten hyperbola obtained with calcium ions can be explained by at least two mechanisms. First, it is possible that both free ATP and ATP-Ca^{2+} complexes are present in these reaction mixtures, whereas in the presence of Mg^{2+} or Mn^{2+}, all of the ATP would be coordinated to a divalent metal ion. The presence of multiple ATP species in the Ca^{2+} mixtures could influence the reaction's course. Second, Ca^{2+} ions may bind to a unique (specific) site in the *Af*GcHK protein that regulates the autophosphorylation reaction. Autophosphorylation in the absence of divalent cations is slower, but the enzyme retains a degree of basal activity under such conditions, suggesting that the absence of a metal cation reduces but does not eliminate its affinity for ATP. The inhibitory divalent metal cations probably bind to sites that are important for catalysis in addition to the enzyme-bound ATP moiety.

SUMMARY

In summary, our results suggest that the heme configuration of *Af*GcHK plays a vital role in regulating its histidine kinase autophosphorylation activity by changing its affinity for ATP, as revealed by changes in its K_m^{ATP} value. This in turn affects the enzyme's catalytic activity, which was quantified in terms of its k_{cat}/K_m^{ATP} value. Figure 8 shows a schematic representation illustrating the effects of changes in the sensor domain heme's redox and coordination states on the activity of the functional domain. It was also shown that the RR-binding site is probably located close to the ATP-binding site of the full-length *Af*GcHK protein because the presence of the RR protein affected the enzyme's K_m^{ATP} value. The results of our kinetic investigations have thus shed new light on the molecular mechanism of the heme-regulated histidine kinase autophosphorylation reaction of *Af*GcHK.

ASSOCIATED CONTENT

Supporting Information

Double reciprocal plots used to determine the enzyme's Michaelis−Menten kinetic parameters, kinetics of CO rebinding in *Af*GcHK proteins and atomic absorption spectroscopy results for WT *Af*GcHK (in its native form). The Supporting Information is available free of charge on the ACS Publications website at DOI: 10.1021/acs.biochem.5b00517.

(PDF)

AUTHOR INFORMATION

Corresponding Author

*Department of Biochemistry, Faculty of Science, Charles University in Prague, Hlavova (Albertov) 2030-8, Prague 2, Czech Republic. Telephone: +420 2 21951242. Fax: +420 2 21951283. E-mail: marketa.martinkova@natur.cuni.cz.

Funding

This work was supported in part by Charles University in Prague (UNCE 204025/2012), by the Grant Agency of the Czech Republic (Grant 15-19883S), and by the Grant Agency of Charles University in Prague (Grants 756214 and 362115).

Notes

The authors declare no competing financial interest.

Dedication

Dedicated to the 65th birthday of Prof. Marie Stiborová.

ABBREVIATIONS

*Af*GcHK, globin-coupled histidine kinase from *Anaeromyxobacter* sp. Fw109-5; P-*Af*GcHK, phosphoform of *Af*GcHK; *Ec* DOS, *E. coli* direct oxygen sensor or heme-regulated phosphodiesterase from *E. coli* or *Ec* DosP; Fe(III), Fe(III)-protoporphyrin IX complex, or hemin; Fe(II), Fe(II)-protoporphyrin IX complex; FixL, oxygen sensor histidine kinase with the heme-bound PAS domain that regulates nitrogen fixation in *R. meliloti* or *Bradyrhizobium japonicum*; GAF, domain conserved in cyclic GMP-specific and stimulated phosphodiesterases, adenylate cyclases, and *E. coli* formate hydrogenlyase transcriptional activator; PAS, acronym from Per (*Drosophila* period clock protein)-Arnt (vertebrate aryl hydrocarbon receptor nuclear translocator)-Sim (*Drosophila* single-minded protein); RR, response regulator; YddV, heme-bound diguanylate cyclase from *E. coli* or *Ec* DosC; WT, wild type.

REFERENCES

(1) Shimizu, T., Huang, D., Yan, F., Stranava, M., Bartosova, M., Fojtíková, V., and Martínková, M. (2015) Gaseous O_2, NO, and CO in signal transduction: Structure and function relationships of heme-based gas sensors and heme-redox sensors. *Chem. Rev. 115*, 6491−6533.

(2) Igarashi, J., Kitanishi, K., and Shimizu, T. (2011) Emerging roles of heme as a signal and a gas-sending site: Heme-sensing and gas-sending proteins. In *Handbook of Porphyrin Science* (Kadish, K. M., Smith, K. M., and Guilard, R., Eds.) Vol. *15*, pp 399−460, World Scientific Publishing, Hackensack, NJ.

(3) Green, J., Crack, J. C., Thomson, A. J., and LeBrun, N. E. (2009) Bacterial sensors of oxygen. *Curr. Opin. Microbiol. 12*, 145−151.

(4) Gilles-Gonzalez, M.-A., and Gonzalez, G. (2005) Heme-based sensors: defining characteristics, recent developments, and regulatory hypotheses. *J. Inorg. Biochem. 99*, 1−22.

(5) Gilles-Gonzalez, M.-A., and Gonzalez, G. (2004) Signal transduction by heme-containing PAS-domain proteins. *J. Appl. Physiol. 96*, 774−783.

(6) Nakamura, H., Kumita, H., Imai, K., Iizuka, T., and Shiro, Y. (2004) ADP reduces the oxygen-binding affinity of a sensory histidine kinase, FixL: the possibility of an enhanced reciprocating kinase reaction. *Proc. Natl. Acad. Sci. U. S. A. 101*, 2742−2746.

(7) Uchida, T., and Kitagawa, T. (2005) Mechanism for transduction of the ligand-binding signal in heme-based gas sensory proteins revealed by resonance Raman spectroscopy. *Acc. Chem. Res. 38*, 662−670.

DOI: 10.1021/acs.biochem.5b00517
Biochemistry 2015, 54, 5017−5029

(8) Sardiwal, S., Kendall, S. L., Movahedzadeh, F., Rison, S. C. G., Stoker, N. G., and Djordjevic, S. (2005) A GAF domain in the hypoxia/NO-inducible *Mycobacterium tuberculosis* DosS protein binds haem. *J. Mol. Biol. 353*, 929−936.
(9) Ioanoviciu, A., Yukl, E. T., Moënne-Loccoz, P., and Ortiz de Montellano, P. R. (2007) DevS, a heme-containing two-component oxygen sensor of *Mycobacterium tuberculosis*. *Biochemistry 46*, 4250−4260.
(10) Sousa, E. H. S., Tuckerman, J. R., Gonzalez, G., and Gilles-Gonzalez, M.-A. (2007) DosT and DevS are oxygen-switched kinases in *Mycobacterium tuberculosis*. *Protein Sci. 16*, 1708−1719.
(11) Kumar, A., Toledo, J. C., Patel, R. P., Lancaster, J. R., and Steyn, A. J. C. (2007) *Mycobacterium tuberculosis* DosS is a redox sensor and DosT is a hypoxia sensor. *Proc. Natl. Acad. Sci. U. S. A. 104*, 11568−11573.
(12) Boon, E. M., and Marletta, M. A. (2005) Ligand specificity of H-NOX domains: from sGC to bacterial NO sensors. *J. Inorg. Biochem. 99*, 892−902.
(13) Ito, Y., Nakagawa, S., Komagata, A., Ikeda-Saito, M., Shiro, Y., and Nakamura, H. (2009) Heme-dependent autophosphorylation of a heme sensor kinase, ChrS, from *Corynebacterium diphtheriae* reconstituted in proteoliposomes. *FEBS Lett. 583*, 2244−2248.
(14) Kitanishi, K., Kobayashi, K., Uchida, T., Ishimori, K., Igarashi, J., and Shimizu, T. (2011) Identification and functional and spectral characterization of a globin-coupled histidine kinase from *Anaeromyxobacter* sp. Fw109−5. *J. Biol. Chem. 286*, 35522−35534.
(15) Inouye, M., and Dutta, R. (2003) *Histidine Kinases in Signal Transduction*, Academic Press, Inc., San Diego.
(16) Kramer, R., and Jung, K. (2010) *Bacterial Signaling*, Wiley-VCH, Weinheim, Germany.
(17) Casino, P., Rubio, V., and Marina, A. (2010) The mechanism of signal transduction by two-component systems. *Curr. Opin. Struct. Biol. 20*, 763−771.
(18) Cheung, J., and Hendrickson, W. A. (2010) Sensor domains of two-component regulatory systems. *Curr. Opin. Microbiol. 13*, 116−123.
(19) Gao, R., Mack, T. R., and Stock, A. M. (2007) Bacterial response regulators: versatile regulatory strategies from common domains. *Trends Biochem. Sci. 32*, 225−234.
(20) Galperin, M. Y. (2010) Diversity of structure and function of response regulator output domains. *Curr. Opin. Microbiol. 13*, 150−159.
(21) Jenal, U., and Galperin, M. Y. (2009) Single domain response regulators: molecular switches with emerging roles in cell organization and dynamics. *Curr. Opin. Microbiol. 12*, 152−160.
(22) Martínková, M., Kitanishi, K., and Shimizu, T. (2013) Heme-based globin-coupled oxygen sensors: linking oxygen binding to functional regulation of diguanylate cyclase, histidine kinase, and methyl-accepting chemotaxis. *J. Biol. Chem. 288*, 27702−27711.
(23) Igarashi, J., Kitanishi, K., Martinkova, M., Murase, M., Iizuka, A., and Shimizu, T. (2008) The roles of thiolate-heme proteins, other than the P450 cytochromes, in the regulation of heme-sensor proteins. *Acta Chim. Slov. 55*, 67−74.
(24) Igarashi, J., Murase, M., Iizuka, A., Pichierri, F., Martinkova, M., and Shimizu, T. (2008) Elucidation of the heme binding site of heme-regulated eukaryotic initiation factor 2alpha kinase and the role of the regulatory motif in heme sensing by spectroscopic and catalytic studies of mutant proteins. *J. Biol. Chem. 283*, 18782−18791.
(25) Anzenbacher, P., Marchal, S., Palacký, J., Anzenbacherová, E., Domaschke, T., Lange, R., Shimizu, T., Kitanishi, K., Stranava, M., Stiborová, M., and Martinkova, M. (2014) Pressure effects reveal that changes in the redox states of the heme iron complexes in the sensor domains of two heme-based oxygen sensor proteins, *Ec*DOS and YddV, have profound effects on their flexibility. *FEBS J. 281*, 5208−5219.
(26) Zhang, W., and Phillips, G. N. (2003) Structure of the oxygen sensor in *Bacillus subtilis*: signal transduction of chemotaxis by control of symmetry. *Structure 11*, 1097−1110.
(27) Yamada, S., Sugimoto, H., Kobayashi, M., Ohno, A., Nakamura, H., and Shiro, Y. (2009) Structure of PAS-linked histidine kinase and the response regulator complex. *Structure 17*, 1333−1344.
(28) Antonini, E., and Brunori, M. (1971) *Hemoglobin and Myoglobin in Their Reactions with Ligands*, North-Holland Publishing Co., Amsterdam.
(29) Fanelli, A. R., Antonini, E., and Caputo, A. (1958) Studies on the structure of hemoglobin. I. Physicochemical properties of human globin. *Biochim. Biophys. Acta 30*, 608−615.
(30) Lobato, L., Bouzhir-Sima, L., Yamashita, T., Wilson, M. T., Vos, M. H., and Liebl, U. (2014) Dynamics of the heme-binding bacterial gas-sensing dissimilative nitrate respiration regulator (DNR) and activation barriers for ligand binding and escape. *J. Biol. Chem. 289*, 26514−26524.
(31) Yamada, S., Nakamura, H., Kinoshita, E., Kinoshita-Kikuta, E., Koike, T., and Shiro, Y. (2007) Separation of a phosphorylated histidine protein using phosphate affinity polyacrylamide gel electrophoresis. *Anal. Biochem. 360*, 160−162.
(32) Gilles-Gonzalez, M. A., and Gonzalez, G. (1993) Regulation of the kinase activity of heme protein FixL from the two-component system FixL/FixJ of *Rhizobium meliloti*. *J. Biol. Chem. 268*, 16293−16297.
(33) Vos, M. H. (2008) Ultrafast dynamics of ligands within heme proteins. *Biochim. Biophys. Acta, Bioenerg. 1777*, 15−31.
(34) Kumazaki, S., Nakajima, H., Sakaguchi, T., Nakagawa, E., Shinohara, H., Yoshihara, K., and Aono, S. (2000) Dissociation and recombination between ligands and heme in a CO-sensing transcriptional activator CooA. A flash photolysis study. *J. Biol. Chem. 275*, 38378−38383.
(35) Kapetanaki, S. M., Field, S. J., Hughes, R. J. L., Watmough, N. J., Liebl, U., and Vos, M. H. (2008) Ultrafast ligand binding dynamics in the active site of native bacterial nitric oxide reductase. *Biochim. Biophys. Acta, Bioenerg. 1777*, 919−924.
(36) Vos, M. H., Bouzhir-Sima, L., Lambry, J.-C., Luo, H., Eaton-Rye, J. J., Ioanoviciu, A., Ortiz de Montellano, P. R., and Liebl, U. (2012) Ultrafast ligand dynamics in the heme-based GAF sensor domains of the histidine kinases DosS and DosT from *Mycobacterium tuberculosis*. *Biochemistry 51*, 159−166.
(37) Feis, A., Lapini, A., Catacchio, B., Brogioni, S., Foggi, P., Chiancone, E., Boffi, A., and Smulevich, G. (2008) Unusually strong H-bonding to the heme ligand and fast geminate recombination dynamics of the carbon monoxide complex of *Bacillus subtilis* truncated hemoglobin. *Biochemistry 47*, 902−910.
(38) Jasaitis, A., Ouellet, H., Lambry, J. C., Martin, J. L., Friedman, J. M., Guertin, M., and Vos, M. H. (2012) Ultrafast heme-ligand recombination in a truncated hemoglobin: a ligand cage. *Chem. Phys. 396*, 10−16.
(39) Silkstone, G., Jasaitis, A., Wilson, M. T., and Vos, M. H. (2007) Ligand dynamics in an electron transfer protein. Picosecond geminate recombination of carbon monoxide to heme in mutant forms of cytochrome *c*. *J. Biol. Chem. 282*, 1638−1649.
(40) Jasaitis, A., Hola, K., Bouzhir-Sima, L., Lambry, J.-C., Balland, V., Vos, M. H., and Liebl, U. (2006) Role of distal arginine in early sensing intermediates in the heme domain of the oxygen sensor FixL. *Biochemistry 45*, 6018−6026.
(41) Yamashita, T., Bouzhir-Sima, L., Lambry, J.-C., Liebl, U., and Vos, M. H. (2008) Ligand dynamics and early signaling events in the heme domain of the sensor protein Dos from *Escherichia coli*. *J. Biol. Chem. 283*, 2344−2352.
(42) Lechauve, C., Bouzhir-Sima, L., Yamashita, T., Marden, M. C., Vos, M. H., Liebl, U., and Kiger, L. (2009) Heme ligand binding properties and intradimer interactions in the full-length sensor protein Dos from *Escherichia coli* and its isolated heme domain. *J. Biol. Chem. 284*, 36146−36159.
(43) Kruglik, S. G., Jasaitis, A., Hola, K., Yamashita, T., Liebl, U., Martin, J.-L., and Vos, M. H. (2007) Subpicosecond oxygen trapping in the heme pocket of the oxygen sensor FixL observed by time-resolved resonance Raman spectroscopy. *Proc. Natl. Acad. Sci. U. S. A. 104*, 7408−7413.

DOI: 10.1021/acs.biochem.5b00517
Biochemistry 2015, 54, 5017−5029

(44) Ye, X., Demidov, A., and Champion, P. M. (2002) Measurements of the photodissociation quantum yields of MbNO and MbO_2 and the vibrational relaxation of the six-coordinate heme species. *J. Am. Chem. Soc. 124*, 5914−5924.
(45) Huang, J. M., Wei, Y. F., Kim, Y. H., Osterberg, L., and Matthews, H. R. (1991) Purification of a protein histidine kinase from the yeast *Saccharomyces cerevisiae*. The first member of this class of protein kinases. *J. Biol. Chem. 266*, 9023−9031.
(46) Conley, M. P., Berg, H. C., Tawa, P., Stewart, R. C., Ellefson, D. D., and Wolfe, A. J. (1994) pH dependence of CheA autophosphorylation in *Escherichia coli*. *J. Bacteriol. 176*, 3870−3877.
(47) Casino, P., Miguel-Romero, L., and Marina, A. (2014) Visualizing autophosphorylation in histidine kinases. *Nat. Commun. 5*, 3258.
(48) Tanaka, A., Takahashi, H., and Shimizu, T. (2007) Critical role of the heme axial ligand, Met95, in locking catalysis of the phosphodiesterase from *Escherichia coli* (*Ec* DOS) toward cyclic diGMP. *J. Biol. Chem. 282*, 21301−21307.
(49) Tanaka, A., and Shimizu, T. (2008) Ligand binding to the Fe(III)-protoporphyrin IX complex of phosphodiesterase from *Escherichia coli* (*Ec* DOS) markedly enhances catalysis of cyclic di-GMP: roles of Met95, Arg97, and Phe113 of the putative heme distal side in catalytic regulation and ligand binding. *Biochemistry 47*, 13438−13446.
(50) Nakajima, K., Kitanishi, K., Kobayashi, K., Kobayashi, N., Igarashi, J., and Shimizu, T. (2012) Leu65 in the heme distal side is critical for the stability of the Fe(II)-O_2 complex of YddV, a globin-coupled oxygen sensor diguanylate cyclase. *J. Inorg. Biochem. 108*, 163−170.
(51) Kitanishi, K., Kobayashi, K., Kawamura, Y., Ishigami, I., Ogura, T., Nakajima, K., Igarashi, J., Tanaka, A., and Shimizu, T. (2010) Important roles of Tyr43 at the putative heme distal side in the oxygen recognition and stability of the Fe(II)-O_2 complex of YddV, a globin-coupled heme-based oxygen sensor diguanylate cyclase. *Biochemistry 49*, 10381−10393.
(52) Liebl, U., Bouzhir-Sima, L., Kiger, L., Marden, M. C., Lambry, J.-C., Négrerie, M., and Vos, M. H. (2003) Ligand binding dynamics to the heme domain of the oxygen sensor Dos from *Escherichia coli*. *Biochemistry 42*, 6527−6535.
(53) Liebl, U., Bouzhir-Sima, L., Negrerie, M., Martin, J.-L., and Vos, M. H. (2002) Ultrafast ligand rebinding in the heme domain of the oxygen sensors FixL and Dos: general regulatory implications for heme-based sensors. *Proc. Natl. Acad. Sci. U. S. A. 99*, 12771−12776.
(54) Liebl, U., Lambry, J.-C., and Vos, M. H. (2013) Primary processes in heme-based sensor proteins. *Biochim. Biophys. Acta, Proteins Proteomics 1834*, 1684−1692.
(55) Chang, A. L., Tuckerman, J. R., Gonzalez, G., Mayer, R., Weinhouse, H., Volman, G., Amikam, D., Benziman, M., and Gilles-Gonzalez, M. A. (2001) Phosphodiesterase A1, a regulator of cellulose synthesis in *Acetobacter xylinum*, is a heme-based sensor. *Biochemistry 40*, 3420−3426.
(56) Roy, J., Sen Santara, S., Bose, M., Mukherjee, S., Saha, R., and Adak, S. (2014) The ferrous-dioxy complex of *Leishmania major* globin coupled heme containing adenylate cyclase: the role of proximal histidine on its stability. *Biochim. Biophys. Acta, Proteins Proteomics 1844*, 615−622.
(57) Levit, M., Liu, Y., Surette, M., and Stock, J. (1996) Active site interference and asymmetric activation in the chemotaxis protein histidine kinase CheA. *J. Biol. Chem. 271*, 32057−32063.
(58) Gilles-Gonzalez, M. A., Gonzalez, G., Perutz, M. F., Kiger, L., Marden, M. C., and Poyart, C. (1994) Heme-based sensors, exemplified by the kinase FixL, are a new class of heme protein with distinctive ligand binding and autoxidation. *Biochemistry 33*, 8067−8073.
(59) Gilles-González, M. A., González, G., and Perutz, M. F. (1995) Kinase activity of oxygen sensor FixL depends on the spin state of its heme iron. *Biochemistry 34*, 232−236.
(60) Foster, J. E., Sheng, Q., McClain, J. R., Bures, M., Nicas, T. I., Henry, K., Winkler, M. E., and Gilmour, R. (2004) Kinetic and mechanistic analyses of new classes of inhibitors of two-component signal transduction systems using a coupled assay containing HpkA-DrrA from *Thermotoga maritima*. *Microbiology 150*, 885−896.
(61) Möglich, A., Ayers, R. A., and Moffat, K. (2009) Design and signaling mechanism of light-regulated histidine kinases. *J. Mol. Biol. 385*, 1433−1444.
(62) Hanna, I. H., Dawling, S., Roodi, N., Guengerich, F. P., and Parl, F. F. (2000) Cytochrome P450 1B1 (CYP1B1) pharmacogenetics: association of polymorphisms with functional differences in estrogen hydroxylation activity. *Cancer Res. 60*, 3440−3444.
(63) Bennett, B. D., Kimball, E. H., Gao, M., Osterhout, R., Van Dien, S. J., and Rabinowitz, J. D. (2009) Absolute metabolite concentrations and implied enzyme active site occupancy in *Escherichia coli*. *Nat. Chem. Biol. 5*, 593−599.
(64) Lowry, O. H., Carter, J., Ward, J. B., and Glaser, L. (1971) The effect of carbon and nitrogen sources on the level of metabolic intermediates in *Escherichia coli*. *J. Biol. Chem. 246*, 6511−6521.
(65) Koç, A., Wheeler, L. J., Mathews, C. K., and Merrill, G. F. (2004) Hydroxyurea arrests DNA replication by a mechanism that preserves basal dNTP pools. *J. Biol. Chem. 279*, 223−230.
(66) Cohen, P. (2000) The regulation of protein function by multisite phosphorylation–a 25 year update. *Trends Biochem. Sci. 25*, 596−601.
(67) Gani, D., and Wilkie, J. (1997) Metal ions in the mechanism of enzyme-catalyzed phosphate monoester hydrolysis. In *Metal Sites in Proteins and Models: Phosphatases, Lewis Acids and Vanadium* (Hill, H. A. O., Sadler, P. J., and Thomson, A. J., Eds.) pp 133−175, Springer-Verlag, Berlin.
(68) Johnson, L. N., and Lewis, R. J. (2001) Structural basis for control by phosphorylation. *Chem. Rev. 101*, 2209−2242.
(69) Shimizu, T. (2013) The heme-based oxygen-sensor phosphodiesterase *Ec* DOS (DosP): Structure-function relationships. *Biosensors 3*, 211−237.
(70) Honjo, A., Takahashi, H., Sekimoto, M., Igarashi, J., and Shimizu, T. (2012) Novel effects of Mn^{2+} on the catalytic enhancement of the inactive form of the Fe(III) heme-bound *Ec* DOS, a heme-regulated phosphodiesterase from *Escherichia coli*. In *Gas Sensors: Developments, Efficacy and Safety* (Qin, X., Ed.) pp 251−261, Nova Science, Hauppauge, NY.

DOI: 10.1021/acs.biochem.5b00517
Biochemistry 2015, 54, 5017−5029